Journal of Thermal Engineering
Yildiz Technical University Press, Istanbul, Turkey
Vol. 2, No. 1, pp.541-549, January, 2016.

http://eds.yildiz.edu.tr/journal-of-thermal-engineering/Articles
Manuscript Received March 17, 2015; Accepted April 27, 2015

This paper was recommended for publication in revised form by Regional Editor Hafiz Muhammad Ali

ENERGY AND EXERGY ANALYSIS OF A DOUBLE EFFECT PARALLEL FLOW LIBR/H_2O ABSORPTION REFRIGERATION SYSTEM

Akhilesh Arora
Department of Mechanical Engineering, Delhi Technological University
Delhi, Delhi, India

***Manoj Dixit**
Centre for Energy Studies, Indian Institute of Technology Delhi
New Delhi, Delhi, India

S.C. Kaushik
Centre for Energy Studies, Indian Institute of Technology Delhi
New Delhi, Delhi, India

Keywords: Parallel flow, Absorption system, Exergy, Exergetic efficiency, Solution distribution ratio.
* *Corresponding author:* Phone: 91-9540660289
E-mail address: mandix@ces.iitd.ac.in

ABSTRACT

In the present communication the analysis of a parallel flow double effect absorption refrigeration system is performed to compute the optimum solution distribution ratio (optimum distribution of strong solution masses between low and high pressure generators) from the viewpoint of maximum COP and maximum exergetic efficiency. A computational model is developed for the parametric investigation of a double effect parallel flow LiBr/H_2O absorption refrigeration system. The effect of generator, absorber and evaporator temperatures on optimum solution distribution ratio is also studied. The results show that the maximum COP and maximum exergetic efficiency is achieved corresponding to same value of optimum solution distribution ratio.

INTRODUCTION

Most absorption cooling systems adopt the double-effect cycle to increase the cooling performance of the system when the heat source available is at high temperature with water lithium bromide. However, when using series flow double effect system the range of operation comes close to the crystallization line of the LiBr solution and the absorption ability becomes weak. The parallel-flow type of double-effect cycle has been proposed to eliminate these difficulties compared with the series-flow type. Compared to the series-flow type, the range of operating conditions of the parallel-flow type is far away from the crystallization line of the LiBr solution, but the control and regulation of the flow rate of solutions are complicated. Many studies are available in literature [1-12] on the first law performance evaluation of both series and parallel flow double effect absorption refrigeration systems. Most of these studies examined the effect of operating parameters like temperatures, solution circulation ratio, and effectiveness of heat exchangers on the system performance. The maximum cop of parallel flow double effect system depends on the optimum distribution of solution, leaving the absorber, between high and low temperature generators. In some of these studies [5, 7, 9] the effect of solution distribution ratio on the cop and cooling capacity has been discussed but the analysis does not include the effect of variation in parameters on optimum value of solution distribution ratio. Lee and Sherif [13], Izquierdo et al. [14] and lee and Sherif [15] are among the earliest researchers who presented the performance analysis of absorption systems based on second law of thermodynamics. Gebreslassie et al. [16] carried out the exergy analysis, considering only unavoidable exergy destruction, for single, double, triple and half effect water-lithium bromide absorption cooling cycles. Izquierdo et al. [17] designed experimental prototype of 7 kW of cooling power. A new type of flat-sheet adiabatic absorber was used to operate at outdoor temperatures of about 45 °c without any sign of crystallization. Exergoeconomic analyses is carried out by Farshi et al. [18] for three types of double effect LiBr-water absorption cooling systems to assess the influence of

various operating parameters on investment cost. Li et al. [19] did the performance analysis of solar air cooled double effect LiBr/H_2O absorption refrigeration system.

It is to be noted that in all the studies mentioned above the optimum solution distribution ratio is not computed corresponding to maximum exergetic efficiency. It is important to determine optimum solution distribution ratio corresponding to maximum exergetic efficiency because minimum irreversibility occurs in a thermal system corresponding to maximum exergetic efficiency.

Keeping this viewpoint, in the present communication the analysis of a parallel flow double effect absorption refrigeration system is performed to compute the optimum solution distribution ratio from the viewpoint of maximum cop and maximum exergetic efficiency. The effect of operating parameters such as generator, absorber and evaporator temperatures is also presented on optimum solution distribution ratio.

MODELLING OF LiBr / H_2O DOUBLE EFFECT PARALLEL FLOW ABSORPTION SYSTEM

Description of the system

Fig. 1 shows schematic diagram of a LiBr/H_2O parallel-flow, double-effect refrigeration system. It includes the most important components of the double-effect cycle: absorber (a), evaporator (e), HP generator (hpg), LP generator (lpg), condenser (c), HT heat exchanger (she_2), LT heat exchanger (she_1) and a solution pump (p). The strong (in absorbent) solution produced in the absorber is separated at the outlet of the LT heat exchanger and is distributed separately to the HP and LP generators. This is the main feature of the parallel-flow double effect absorption refrigeration system. The ratio of solution entering the HP generator to the solution leaving the solution pump is known as solution distribution ratio. The solution in the high-pressure generator is heated externally from solar energy or waste heat or any other heat source. The refrigerant vapour (steam) produced in the HP generator is used as a heat source for the low-pressure generator. The weak (in refrigerant) solution from the HP generator passes through the HT heat exchanger and mixes with the weak solution coming from LP generator through the solution throttle valve (stv_2) at the inlet of the LT heat exchanger. The solution then enters the absorber and is diluted by absorbing the refrigerant vapour coming from evaporator. The refrigerant vapour produced by the LP generator is condensed in the condenser, and flows to the evaporator. The refrigerant generated in LP and HP generators mix before entering the evaporator. In evaporator, liquid refrigerant extracts heat from the space to be cooled and evaporates, thereby producing cooling effect.

Mathematical Modelling

The thermodynamic analysis of the system involves the application of principles of mass conservation, species conservation, energy balance and exergy balance to individual components of the system. Mass and species conservation for each component can be written in general form as follows:

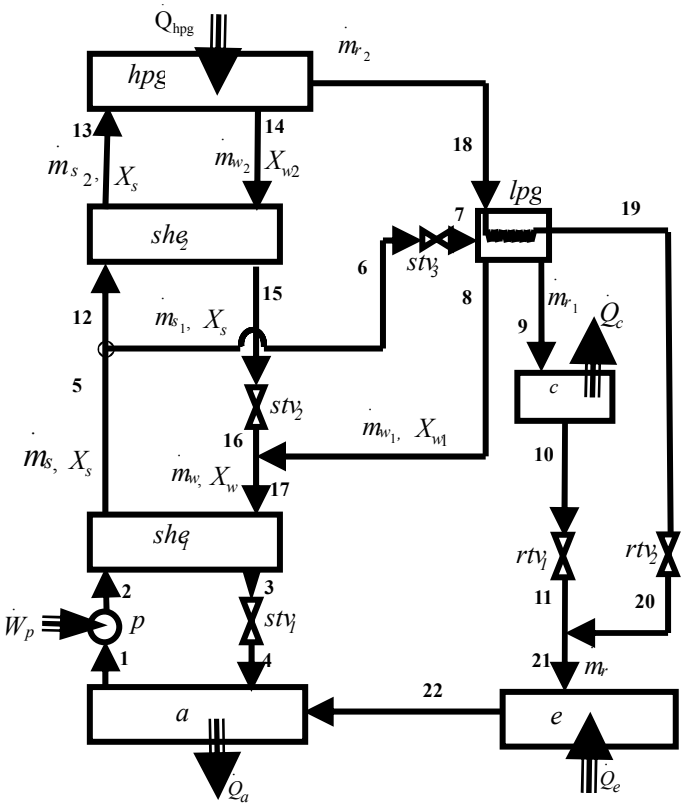

Fig. 1. Schematic diagram of a Parallel Flow Double Effect Absorption Refrigeration System

$$\Sigma \dot{m}_i = \Sigma \dot{m}_e \quad (1)$$

$$\Sigma \dot{m}_i \, X_i = \Sigma \dot{m}_e \, X_e \quad (2)$$

The energy balance of the system is specified by equation (3).

$$\Sigma \dot{Q} - \Sigma \dot{W} = \Sigma \dot{m}_e \, h_e - \Sigma \dot{m}_i \, h_i \quad (3)$$

Properties at various state points are calculated using the equations (4) to (10).

LiBr/H_2O solution: $f_1 (h, X, T) = 0$ (4)

$f_2 (s, X, T) = 0$ (5)

$f_3 (P, T, X) = 0$ (6)

Refrigerant (water): $f_4 (h, P, T) = 0$ (7)

$f_5 (s, P, T) = 0$ (8)

$f_6 (h, T_{sat}) = 0$ (9)

$f_7 (s, T_{sat}) = 0$ (10)

Exergy is the property of a system relative to a reference state, which gives the maximum power that can be extracted from the system when it is brought in to thermodynamic equilibrium with the reference state [20]. Exergy balance for a control volume undergoing steady state process is expressed as [13].

$$\dot{E}D_t = \sum\left(\dot{m}e\right)_{in} - \sum\left(\dot{m}e\right)_{out} + \left[\sum\left(\dot{Q}\left(1-\frac{T_0}{T}\right)\right)_{in} - \sum\left(\dot{Q}\left(1-\frac{T_0}{T}\right)\right)_{out}\right] \pm \sum\dot{W} \quad (11)$$

where $\dot{E}D_i$ represents the rate of exergy destruction or the irreversibility occurring in the process. The first two terms on the right hand side represent exergy of streams entering and leaving the control volume. The third and fourth terms are the exergy associated with heat transfer $\dot{Q}$ from the source maintained at constant temperature T and is equal to work obtained by Carnot engine operating between T and T_0, and is therefore equal to maximum reversible work that can be obtained from heat energy $\dot{Q}$. The last term is the mechanical work transfer to or from the control volume.

Second law performance of the system can be measured in terms of exergetic efficiency [21]. It is defined as the useful exergy or available energy gained from a system to that supplied to the system. For the double effect system under consideration, it is the ratio of the exergy of the cooling effect produced by the evaporator to the exergy of the heat supplied at the HP generator plus pump work supplied.

$$\eta_{ex} = \frac{E\dot{Q}_e}{E\dot{Q}_{hpg} + \dot{W}_p} = 1 - \frac{\dot{E}D_t}{E\dot{Q}_{hpg} + \dot{W}_p} \quad (12)$$

The above modeling procedure forms the basis for the equations given in the subsequent paragraph.

Mass, material and energy balance of parallel flow double effect absorption refrigeration system

The mass and material balance at high temperature generator, second effect generator and condenser are given by:

HP Generator

$$\dot{m}_{s_2} = \dot{m}_{r_2} + \dot{m}_{w_2} \quad (13)$$

$$\dot{m}_{s_2} X_s = \dot{m}_{w_2} X_{w_2} \quad (14)$$

LP generator

$$\dot{m}_{s_1} = \dot{m}_{r_1} + \dot{m}_{w_1} \quad (15)$$

$$\dot{m}_{s_1} X_s = \dot{m}_{w_1} X_{w_1} \quad (16)$$

Splitter (state points 5-6-12)

$$\dot{m}_s = \dot{m}_{s_1} + \dot{m}_{s_2} \quad (17)$$

Mixer (state points 8-16-17)

$$\dot{m}_w = \dot{m}_{w_1} + \dot{m}_{w_2} \quad (18)$$

$$\dot{m}_w X_w = \dot{m}_{w_1} X_{w_1} + \dot{m}_{w_2} X_{w_2} \quad (19)$$

Mixer (state points 11-20-21)

$$\dot{m}_r = \dot{m}_{r_1} + \dot{m}_{r_2} \quad (20)$$

Solution circulation ratio is specified by equation (21).

$$SCR = \frac{\dot{m}_s}{\dot{m}_r} = \frac{X_w}{X_w - X_s} \quad (21)$$

Solution distribution ratio (R) is specified by equation (22).

$$R = \frac{\dot{m}_{s_2}}{\dot{m}_s} \quad (22)$$

The energy balance in each component of a parallel flow double effect system is given by the following equations:

$$\dot{Q}_a = \dot{m}_r h_{22} + \dot{m}_w h_4 - \dot{m}_s h_1 \quad (23)$$

$$\dot{Q}_{hpg} = \dot{m}_{r_2} h_{18} + \dot{m}_{w_2} h_{14} - \dot{m}_{s_2} h_{13} \quad (24)$$

$$\dot{Q}_{lpg} = \dot{m}_{r_2}(h_{18} - h_{19}) = \dot{m}_{r_1} h_9 + \dot{m}_{w_1} h_8 - \dot{m}_{s_1} h_7 \quad (25)$$

$$\dot{Q}_c = \dot{m}_{r_1}(h_9 - h_{10}) \quad (26)$$

$$\dot{Q}_e = \dot{m}_r (h_{22} - h_{21}) \quad (27)$$

$$\dot{Q}_{she_1} = \dot{m}_s (h_5 - h_2) = \dot{m}_w (h_{17} - h_3) \quad (28)$$

$$\dot{Q}_{she_2} = \dot{m}_{s_2}(h_{13} - h_{12}) = \dot{m}_{w_2}(h_{14} - h_{15}) \quad (29)$$

$$\dot{W}_p = \dot{m}_s(h_2 - h_1) \quad (30)$$

$$\dot{E}_{in} = \dot{Q}_{hpg} + \dot{Q}_e + \dot{W}_p \quad (31)$$

$$\dot{E}_{out} = \dot{Q}_a + \dot{Q}_c \quad (32)$$

$$COP = \frac{\dot{Q}_e}{\dot{Q}_{hpg} + \dot{W}_p} \quad (33)$$

Exergy destruction in each component of a parallel flow double effect absorption refrigeration system is furnished below.

$$\dot{E}D_a = \dot{m}_r(h_{22} - T_o s_{22}) + \dot{m}_w(h_4 - T_o s_4) - \dot{m}_s(h_1 - T_o s_1) - \dot{Q}_a\left(1 - \frac{T_o}{T_a}\right) \quad (34)$$

$$\dot{E}D_{hpg} = \dot{m}_{s_2}(h_{13} - T_o s_{13}) - \dot{m}_{w_2}(h_{14} - T_o s_{14}) - \dot{m}_{r_2}(h_{18} - T_o s_{18}) + \dot{Q}_{hpg}\left((1 - \frac{T_o}{T_{hpg}}\right) \quad (35)$$

$$\dot{E}D_{lpg} = \dot{m}_{s_1}(h_7 - T_o s_7) - \dot{m}_{w_1}(h_8 - T_o s_8) + \dot{m}_{r_2}(h_{18} - T_o s_{18}) - \dot{m}_{r_2}(h_{19} - T_o s_{19}) - \dot{m}_{r_1}(h_9 - T_o s_9) \quad (36)$$

$$\dot{E}D_c = \dot{m}_{r_1}\left((h_9 - h_{10}) - T_o(s_9 - s_{10})\right) - \dot{Q}_c\left(1 - \frac{T_0}{T_c}\right) \quad (37)$$

$$\dot{E}D_e = \dot{m}_r((h_{21} - h_{22}) - T_o(s_{21} - s_{22})) + \dot{Q}_e\left(1 - \frac{T_0}{T_r}\right) \quad (38)$$

$$\dot{E}D_{she_1} = \dot{m}_s((h_2 - h_5) - T_o(s_2 - s_5)) + \dot{m}_w((h_{17} - h_3) - T_o(s_{17} - s_3)) \quad (39)$$

$$\dot{E}D_{she_2} = \dot{m}_{s_2}((h_{12} - h_{13}) - T_o(s_{12} - s_{13})) + \dot{m}_{w_2}((h_{14} - h_{15}) - T_o(s_{14} - s_{15})) \quad (40)$$

$$\dot{E}D_{rtv_1} = \dot{m}_{r_1} T_o(s_{10} - s_{11}) \quad (41)$$

$$\dot{E}D_{rtv_2} = \dot{m}_{r_2} T_o(s_{19} - s_{20}) \quad (42)$$

$$\dot{E}D_{stv_1} = \dot{m}_w T_o(s_3 - s_4) \quad (43)$$

$$\dot{E}D_{stv_2} = \dot{m}_{w_2} T_o(s_{15} - s_{16}) \quad (44)$$

$$\dot{E}D_{stv_3} = \dot{m}_{s_1} T_o(s_6 - s_7) \quad (45)$$

$$\dot{E}D_{mixer_{8-16-17}} = \dot{m}_{w_1}((h_8 - T_0 s_8) + \dot{m}_{w_2}((h_{16} - T_0 s_{16}) - \dot{m}_w((h_{17} - T_0 s_{17}) \quad (46)$$

$$\dot{E}D_{mixer_{11-20-21}} = \dot{m}_{r_1}((h_{11} - T_0 s_{11}) + \dot{m}_{r_2}((h_{20} - T_0 s_{20}) - \dot{m}_r((h_{21} - T_0 s_{21}) \quad (47)$$

$$\dot{E}D_t = \dot{E}D_a + \dot{E}D_{hpg} + \dot{E}D_{lpg} + \dot{E}D_c + \dot{E}D_e + \dot{E}D_{she_1} + \dot{E}D_{she_2} + \dot{E}D_{rtv_1} + \dot{E}D_{rtv_2} + \dot{E}D_{stv_1} + \dot{E}D_{stv_2} + \dot{E}D_{stv_3} + \dot{E}D_{mixer_{8-16-17}} + \dot{E}D_{mixer_{11-20-21}} \quad (48)$$

Equation (12) can now be rewritten in the form as shown in equation (49).

$$\eta_{e_x} = \frac{\dot{Q}_e\left|\left(1 - \frac{T_0}{T_r}\right)\right|}{\dot{Q}_{hpg}\left(1 - \frac{T_0}{T_{hpg}}\right) + \dot{W}_p} \quad (49)$$

RESULTS AND DISCUSSION

The present work is based on the following assumptions:-

1. Pressure and heat losses through the system components are negligible.
2. Solution leaving the absorber and the generator are assumed to be saturated in equilibrium conditions at their respective temperatures and concentrations.
3. Refrigerant leaving the condenser and vapour leaving the evaporator are assumed to be saturated at their respective saturation temperatures.
4. Refrigerant vapour leaving the HP generator is considered to be superheated vapour at the generator temperature.
5. Non equilibrium states at the inlet to the HP generator, and the absorber and states at outlet to the solution pump and the solution heat exchanger are taken to be at their actual conditions.
6. Pumping process is assumed to be reversible adiabatic.
7. Throttling of the refrigerant is assumed to be isenthalpic and non-isentropic while solution throttling is considered to be isothermal, isenthalpic and non-isentropic.

8. The temperature in high temperature heat source, medium temperature heat sink and low temperature heat source are assumed to be constant while the fluid temperature varies in non-isothermal components due to different inlet/outlet solution concentrations.
9. The reference enthalpy (h_o) and entropy (s_o) used for calculating exergy of the working fluid are the values for water at an environment temperature (T_o) of 25°C.
A computer program has been developed using Engineering Equation Solver (EES) software [22] for carrying out the energy and exergy analysis of the single effect and double effect absorption refrigeration systems. The properties of LiBr/H_2O solution used for the analysis purpose have been obtained from correlations developed by Pátek and Klomfar [23]. Subroutines for calculating the properties of LiBr-H_2O solution were linked to the library file of the EES. Following parameters are assumed for parametric computations:-
1. High pressure generator temperature (T_{hpg}) = 120 °C – 170 °C
2. Evaporator temperature (T_e) = 7.2 °C
3. Condenser and absorber temperatures are assumed to be equal. ($T_c = T_a$) = 29.4 °C /37.8 °C
4. Effectiveness of solution heat exchanger(s), (ε) = 0.7
5. Temperature of the space to be cooled (T_r) = 17.2 °C
6. Cooling capacity of the system ($\dot{Q}_e$) = 100 kW

The results computed from the present work are compared with the results given in Riffat and Shankland (1993) and are detailed in Table 1. The difference in values of heat transfers in various components is less than 3%. The difference in value of COP is less than 0.6%.

Table 1. Comparison of present results with the results of Riffat and Shankland [6]

Parameter	Results reported by Riffat and Shankland [6]	Computed results	Difference in reported and Computed values
Heat supplied in HP generator, ($\dot{Q}_{hpg}$), kW	71.2	70.81	-0.55 %
Cooling effect ($\dot{Q}_e$), kW	100	100	---
Heat rejected by the absorber ($\dot{Q}_a$), kW	119.99	121.5	1.26%
Heat rejected by the condenser ($\dot{Q}_c$), kW	51.20	49.32	-3.67%
Pump work ($\dot{W}_p$), kW	0.0	0.0083	----
COP	**1.404**	**1.41**	**0.43%**

Fig. 2 illustrates the effect of variation in solution distribution ratio and HP generator temperature on the COP ($T_c = T_a$ = 29.4 °C). The COP increases with reduction in HP generator temperature. The reason being that for same solution distribution ratio, the increase in HP generator temperature cause an increase in exergy destruction in HP generator, absorber, condenser, LP generator and total exergy destruction. The maximum value of COP varies between 1.39 and 1.42. The global maximum of COP is observed at 135°C HP generator temperature. Further with increase in solution distribution ratio, it is observed that total exergy destruction first decreases up to the optimum and then again starts increasing.

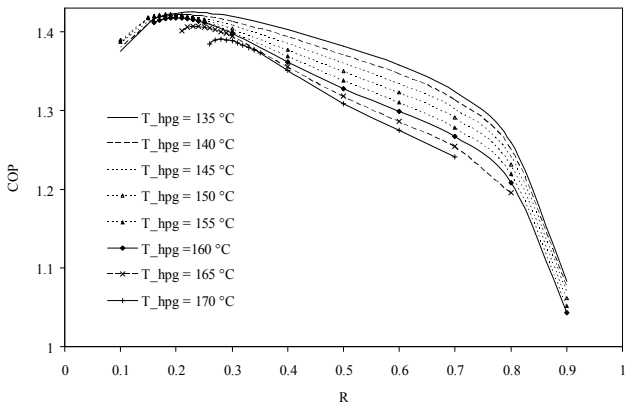

Fig. 2. Effect of solution distribution ratio (R) and high pressure generator temperature on COP (Te=7.2 °C, Ta= Tc=29.4 °C).

The optimum value of solution distribution ratio for maximum COP varies between 0.19 and 0.28 depending upon the HP generator temperature, indicating best results are achieved when most of the solution is distributed to the LP generator and simultaneously minimum total exergy destruction is observed corresponding to these values. Secondly, it is observed that with increase in HP generator temperatures (i.e. between 135 °C to 155 °C) the optimum solution distribution ratio decreases from 0.23 to 0.19 and for temperatures between 155 °C and 170 °C, it increases to 0.28. Moreover lower values of R_{opt} show that circulation losses are also less when lesser amount of solution is entering the HP generator. The nature of the curve obtained in

the present analysis is similar to the curve obtained by Gommed and Grossman [5] in their analysis.

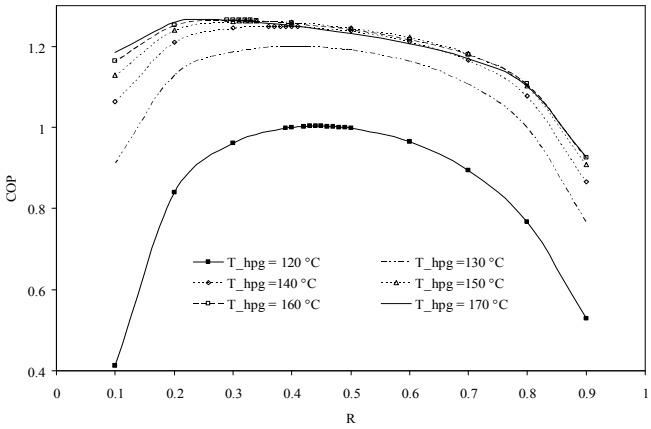

Fig. 3. Effect of solution distribution ratio (R) and high pressure generator temperature on COP (Te=7.2 °C, Ta= Tc=37.8 °C)

Fig. 3 presents the effect of increasing the absorber and condenser temperatures on the COP and optimum solution distribution ratio. It is observed that with increase in the absorber and condenser temperatures (from 29.4 to 37.8 °C), the COP and its maximum value drops for the range of generator temperatures considered. It happens because of increase in solution circulation ratio, with increase in absorber and condenser temperatures, and it causes increase in circulation losses and hence reduction in COP. Further the optimum solution distribution ratio is achieved at higher values of solution distribution ratio than before. It indicates that more solution is required to be pumped to HP generator at higher absorber and condenser temperatures to achieve maximum value of the COP. However increasing the HP generator temperature causes the optimum distribution ratio to shift toward lower values of solution distribution ratio.

Fig. 4 depicts the effect of solution distribution ratio and HP generator temperature on exergetic efficiency. It is observed that increase in the HP generator temperature brings down the exergetic efficiency. The same reasons can be attributed for such a behaviour as already explained for the trend of COP curve. Secondly, with increase in solution distribution ratio, there is increase in exergetic efficiency up to optimum value of solution distribution ratio and beyond which there is drop in exergetic efficiency. The optimum value of solution distribution ratio lies between 0.23 - 0.19 for the HP generator temperatures between 135 °C and 155 °C, and for temperatures above 155 °C and up to 170 °C, it increases to 0.28.

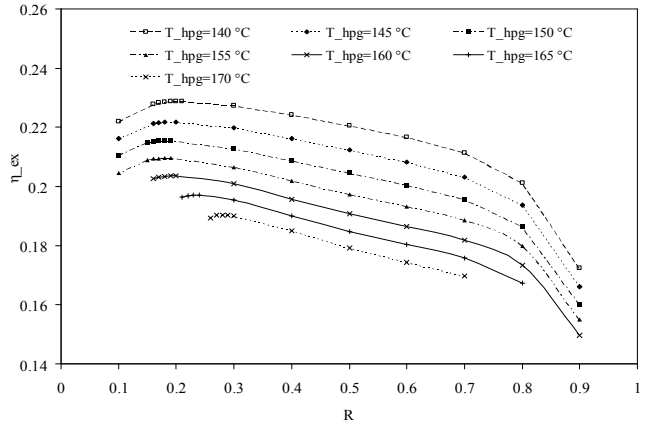

Fig. 4. Effect of solution distribution ratio (R) and high pressure generator temperature on exergetic efficiency (Te=7.2 °C, Ta= Tc=29.4 °C)

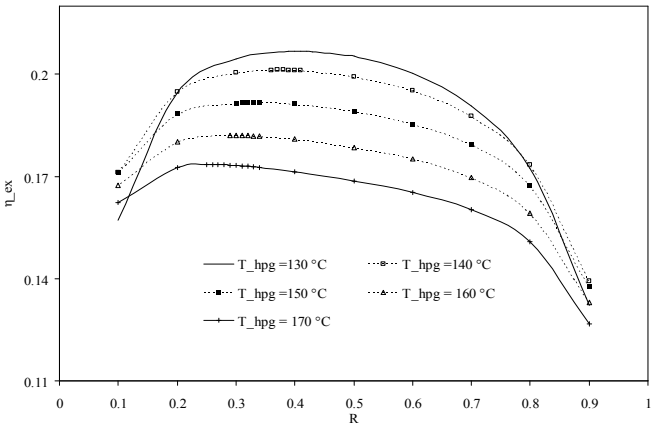

Fig. 5. Effect of solution distribution ratio (R) and high pressure generator temperature on exergetic efficiency (Te=7.2 °C, Ta= Tc=37.8 °C).

The effects of increase in absorber and condenser temperatures on exergetic efficiency and optimum solution distribution ratio are represented in Fig. 5. The increase in the absorber and condenser temperatures is responsible for reduction of exergetic efficiency. It happens because of overall increase in solution circulation ratio with increase in absorber and condenser temperatures which causes increase in circulation losses and irreversibility in various components of the system increase and hence reduction in exergetic efficiency. The higher values of the exegetic efficiency are achieved at lower values of HP generator temperature for solution distribution ratio varying between 0.2 and 0.77. The optimum value of solution distribution ratio increases as compared to the case when absorber and condenser temperatures are lower.

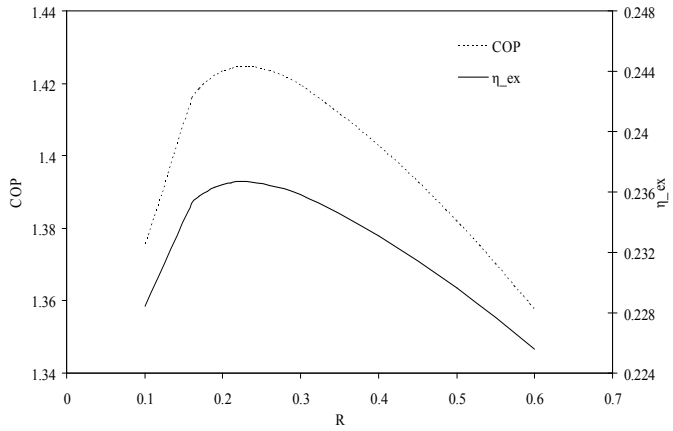

Fig. 6. Variation of COP and exergetic efficiency with solution distribution ratio (R) (T_{hpg}= 135 °C, Te = 7.2 °C, Ta = Tc = 29.4 °C)

Fig. 6 depicts the variation of the COP and exergetic efficiency with solution distribution ratio. It is observed that the maximum value of the COP and exergetic efficiency occur for same solution distribution ratio. This happens because minimum irreversibility occurs at optimum solution distribution ratio. The similar results were also obtained for different values of generator temperature at other absorber and condenser temperatures.

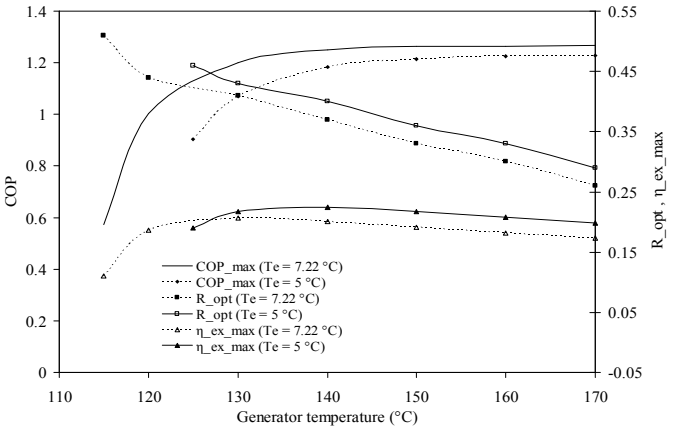

Fig. 7. Variation of maximum COP and exergetic efficiency and R_{opt} with T_{hpg} for varying evaporator temperatures

Fig. 7 shows the effect of variation in the evaporator temperature on the optimum solution distribution ratio, maximum COP and maximum exergetic efficiency at condenser and absorber temperature of 37.8 °C. The overall system irreversibility increases with reduction in evaporator temperature and hence maximum value of the COP and the exergetic efficiency reduce.

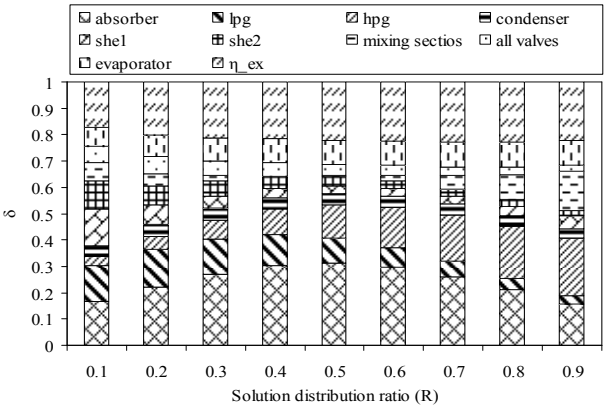

Fig. 8. Exergy destruction in different components at various solution distribution ratios (R)

Fig. 8 represents the variation of exergy destruction in different components with solution distribution ratio at high pressure generator temperature of 140 °C and condenser and absorber temperature of 29.4 °C. It is observed that total exergy destruction is lowest at optimum solution distribution ratio and it increases on either side of the optimum solution distribution ratio on either side. The absorber is the component in which percentage exergy destruction is maximum followed by HP generator, mixing sections, LP generator and evaporator.

CONCLUSIONS

In the present analysis, we have performed the energy and exergy analysis of a parallel flow double effect $LiBr/H_2O$ absorption refrigeration system. The conclusions drawn from this analysis are specified point wise below.

1. The COP and exergetic efficiency increases with reduction in HP generator temperature. Thus global maximum of COP is observed at 135°C HP generator temperature. The maximum value of COP varies between 1.39 and 1.42. The optimum value of solution distribution ratio for maximum COP varies between 0.19 and 0.28 depending upon the HP generator temperature. The optimum value of solution distribution corresponds to minimum exergy destruction.

2. Increasing the absorber and condenser temperatures cause the COP, exergetic efficiency and their maximum values to drop. The optimum solution distribution ratio is achieved at higher values of solution distribution ratio.

3. The maximum values of the COP and exergetic efficiency occur for same solution distribution ratio.

4. The total exergy destruction is lowest at optimum solution distribution ratio and it increases on either side of the optimum solution distribution ratio. The absorber is the component in

which percentage exergy destruction is maximum followed by HP generator, mixing sections, LP generator and evaporator.

NOMENCLATURE

COP	Coefficient of performance
e, E	Specific exergy ($kJkg^{-1}$), Exergy (kJ)
$\dot{E}$	Rate of energy (kW)
$\dot{E}D$	Rate of exergy destruction (kW)
f	Function
h	Specific enthalpy ($kJ\ kg^{-1}$)
HP	High pressure
HT	High temperature
LP	Low pressure
LT	Low temperature
$\dot{m}$	Mass flow rate ($kg\ s^{-1}$)
P	Pressure (kPa)
$\dot{Q}$	Heat transfer rate (kW)
s	Specific entropy ($kJ\ kg^{-1}\ K^{-1}$)
SCR	Solution circulation ratio
R	Solution distribution ratio
T	Temperature (K)
$\dot{W}$	Work transfer rate (kW)
X	LiBr mass fraction
Subscripts	
0	Represents dead state
1, 2, 3…	Represent state points in fig. 1 and 2
a	Absorber
aev	All expansion valves
C	Condenser
e	Evaporator, exit
hpg	High pressure generator
i	Inlet, any component
in	input
lpg	Low pressure generator
max	Maximum
opt	Optimum
out	Out
p	Pump
r	Refrigerant, space to be cooled
rtv	Refrigerant throttle valve
s	Strong
she	Solution heat exchanger
stv	Solution throttle valve
t	Total
w	Weak
Greek letter	
δ	Efficiency defect
ε	Effectiveness of solution heat exchanger(s)
η	Efficiency

ACKNOWLEDGMENTS

The support of Ministry of New and Renewable Energy (MNRE), Government of India is duly acknowledged.

REFERENCES

[1] Vliet G.C., Lawson, M.B., Lithgow, R.A., 1982. Water-Lithium Bromide double effect absorption cooling system analysis. ASHRAE Transactions HO-82-5(2), 811-823.

[2] Fallek M., 1985. Parallel flow Chiller- heater. ASHRAE Transactions HI-85-41(5), 2095-2102.

[3] Kaushik S. C. and Chandra S., 1985. Computer modeling and parametric study of a double effect generation absorption refrigeration cycle. Energy Conversion Management 25(1), 9-14.

[4] Iyer, P. S. A, Murthy S. S. and Murthy M. V. K., 1988. Correlations for evaluation of the performance characteristics of vapour absorption refrigeration cycles. Solar & Wind Technology 5 (2), 191-197.

[5] Gommed K. and Grossman, G., 1990. Performance analysis of staged absorption heat pumps: water-lithium bromide systems. ASHRAE Transactions 30(6), 1590-1598.

[6] Riffat, S. B. and Shankland, N., 1993. Integration of absorption and vapour-compression systems. Applied Energy 46(4), 303-316.

[7] Oh M. D., Kim S. C., Kim Y. L. and Kim Y. I., 1994. Cycle analysis of an air-cooled $LiBr/H_2O$ absorption heat pump of parallel-flow type. International Journal of Refrigeration 17(8), 556- 565.

[8] Xu G. P., Dai Y. Q., Tou K. W. and Tso C. P.,1996. Theoretical analysis and optimization of a double-effect series-flow-type absorption chiller. Applied Thermal Engineering 16(12), 975-987.

[9] Xu G. P. and Dai Y.Q., 1997. Theoretical analysis and optimization of a double-effect parallel flow type absorption chiller. Applied Thermal Engineering 17(2), 157-170.

[10] Arun M.B., Maiya M.P., Murthy S. S, 2000. Equilibrium low pressure generator temperatures for double effect series flow absorption refrigeration systems. Applied Thermal Engineering 20, 227-242.

[11] Elsafty A and Al-Daini A.J., 2000. Theoretical Investigation of a water-lithium bromide vapour absorption cooler, Renewables: The Energy for the 21st Century World Renewable Energy Congress VI, Brighton, UK, 2202-2205.

[12] Arun M.B., Maiya M.P., Murthy S. S, 2001. Performance comparison of double effect parallel flow and series flow water lithium bromide absorption systems. Applied Thermal Engineering 21, 1273-1279.

[13] Lee, S.F., Sherif, S.A., 1999. Second law analysis of multi effect Lithium Bromide/Water absorption chillers. ASHRAE Transactions Ch-99-23(3), 1256- 1266.
[14] Izquierdo M., Vega M. D, Lecuona A., Rodríguez P., 2000. Entropy generated and exergy destroyed in lithium bromide thermal compressors driven by the exhaust gases of an engine. International Journal of Energy Research 24(13**)**, 1123 – 1140.
[15] Lee, S.F., Sherif, S.A., 2001. Second law analysis of various double effect Lithium Bromide/Water absorption chillers. ASHRAE Transactions AT-01-9(5), 664-673.
[16] Gebreslassie B.H., Medrano M., Boer D., 2010. Exergy analysis of multi-effect water LiBr/absorption systems: From half to triple effect. Renewable Energy 35, 1773–1782.
[17] Izquierdo M., Marcos J.D., Palacios M.E., González-Gil A., 2012. Experimental evaluation of a low-power direct air-cooled double-effect LiBr-H2O absorption prototype. Energy 37, 737-748.
[18] Farshi L.G., Mahmoudi S.M.S., Rosen M.A., Yari M., Amidpour M., 2013. Exergoeconomic analysis of double effect absorption refrigeration systems. Energy Conversion and Management 65, 13–25.
[19] Li Z., Ye X., Liu J., 2014. Performance analysis of solar air cooled double effect LiBr/H_2O absorption cooling system in subtropical city. Energy Conversion and Management 85, 302-312.
[20] Arcaklıoğlu E., Cavuşoğlu A. and Erişen A, 2005. An algorithmic approach towards finding better refrigerant substitutes of CFCs in terms of the second law of thermodynamics. Energy Conversion and Management 46, 1595-1611.
[21] Bejan, A., Tsatsaronis, G., Moran, M., 1996. Thermal Design and Optimization. John Wiley and Sons Inc., USA, 143–156.
[22] Klein S.A., Alvarado F., 2005. Engineering Equation Solver, Version 7.441, F-Chart software, Middleton, WI.
[23] Pátek J., Klomfar J., 2006. A computationally effective formulation of the thermodynamic properties of LiBr/H2O solutions from 273 to 500 K over full composition range. International Journal of Refrigeration 29, 566-578.